

SOLAR OPTICAL AND INFRARED RADIATIVE PROPERTIES OF TRANSPARENT POLYMER FILMS

Gernot Wallner, Harald Schobermayr and Reinhold W. Lang

Institute of Polymer Technology, JOANNEUM RESEARCH and Institute of Materials Science and Testing of Plastics, University of Leoben, Franz-Josef-Str. 18, Leoben, A-8700, Austria, +43 3842 402 – 483, Fax – 525, wallner@unileoben.ac.at

Werner J. Platzer

Fraunhofer-Institute for Solar Energy Systems,
Oltmannsstr. 5, Freiburg, D-79100, Germany

Abstract – Polymer films are used in various solar energy devices, such as transparent insulation materials, encapsulation of solar cells, windows, substrates for functional layers, etc. In many cases the radiative properties of the films in the solar and infrared range are of importance for the specific application. This paper describes averaged solar optical and infrared radiative properties for various transparent polymer films including different polymer types and film thicknesses. The measurements were performed from the near ultraviolet to the medium infrared, covering the range of interest for calculating solar and thermal radiative transfer through glazings (e.g., transparent insulation). Concerning the solar optical properties, the extinction is dominated by scattering. In general, semicrystalline polymer films show higher solar losses than amorphous polymer films. Furthermore, additives frequently used in commercial polymer films to improve e.g. manufacturing, tear resistance and weathering behaviour also affect the solar optical properties of polymer films. In the medium infrared range, extinction is caused by absorption due to intramolecular bond rotations and vibrations of molecular groups and segments of polymeric chains. For blackbody temperatures from 10 to 100 °C ether-, fluoride-, imide-, sulphone- and siloxane-groups are of major relevance.

1. INTRODUCTION

Since 1960 transparent polymer films continuously have been gaining importance in a wide range of applications (e.g., packaging, electronic). Many different film types and laminates have been developed. Due to their excellent optical properties (high transparency) and thermal characteristics (low heat conductivity) as well as further polymer-specific advantages (e.g., material properties which can be varied within a wide range; highly flexible processability; high economy) polymer films possess an outstanding potential for many solar applications as well. At present transparent polymer films are already used for encapsulation of photovoltaic (pv) cells, as convection barrier in solar collectors and as substrate or adhesive layer for glazings. Previous research (Platzer, 1992; Rubin, 1982; Neidlinger, 1987; Graf et al., 1985) on radiative properties of films focused on selected polymer types or selected radiation ranges and properties. However, so far no comprehensive investigations have been reported which systematically consider the effects of polymer type and film thickness on the averaged radiative properties in the solar and medium IR range.

Hence, the purpose of this paper is to describe and compare the results obtained for solar optical and infrared radiative properties of various commercial polymer films. In particular, the effects of polymer type and film thickness on the integral radiative properties with the specific view on the use of such polymer films in TI structures, in which repeated interactions

between incoming radiation and successively arranged polymer films take place (i.e., multiple film interactions), will be discussed. The results are interpreted in terms of both the molecular and supermolecular structure of the various polymer film types.

2. BACKGROUND AND METHODOLOGY

At the Institute of Polymer Technology (JOANNEUM RESEARCH Forschungsges.m.b.H, Leoben, Austria) a research project to develop and optimize transparent insulation (TI) structures based on commercially available polymer films was carried out in close cooperation with the Institute of Materials Science and Testing of Plastics (University of Leoben, A) and the Fraunhofer-Institute for Solar Energy Systems (Freiburg, D). For the optimization of the TI structures, 80 different polymer films including film thicknesses ranging from 12 to 150 μm were investigated as to their relevant integral radiative properties (solar extinction coefficient, η^{S} , consisting of the solar scattering coefficient, σ^{S} , and the solar absorption coefficient, κ^{S} ; infrared absorption coefficient, κ_{IR}).

First, a market survey was carried out on commercially available transparent polymer films. Both, commodity plastics with maximum service temperatures of about 100 °C and speciality polymers with long term service temperatures ranging from 150 to 200 °C were considered. In total, more than 20 different types of plastics were selected for the investigations. As to the influence of film thickness, care was taken to select

film types, which were processed from the same moulding compound.

All polymer films were characterized spectroscopically at normal or near-normal incidence and the integral values were calculated based on published theories and formulas. Values for film thickness and the index of refraction over the whole radiation range were taken from data sheets and from the literature. In addition, the thickness of all films was measured with a caliper and by light and scanning electron microscopy.

3. EXPERIMENTAL AND CALCULATION PROCEDURES

3.1 Polymer Film Types

The polymer film types investigated are listed in Table 1 along with the polymer nomenclature and with information as to the polymer morphology (amorphous or semicrystalline), the maximum long term service temperature (based on literature data and producers data sheets), the index of refraction, the film thickness and the film production process (film casting or film extrusion).

3.2 Spectroscopical Characterization

The optical data used for inputs to the calculations were determined using two experimental techniques. Over the solar spectrum from 300 to 2500 nm the collimated-hemispherical and collimated-diffuse transmittance values at normal incidence and

reflectance values at near-normal incidence were determined using a Perkin Elmer Lambda 9 Ulbricht globe spectrophotometer (Perkin Elmer; Überlingen, D). The BaSO₄ coated Ulbricht globe had a diameter of 15 cm. For the given measurement apparatus the radiation passing through the specimen or being reflected by the specimen outside a cone of approximately 5° relative to the incident beam direction is defined as diffuse component. The hemispherical and diffuse values allowed the calculation of both, the extinction coefficient due to absorption and the scattering coefficient (see below).

Over the medium IR range from 180 to 4000 cm⁻¹ (2500 to 5555 nm) the collimated-collimated transmittance spectra at normal incidence were obtained with a Perkin Elmer PE330 grating spectrometer (Perkin Elmer; Überlingen, D). Thus, the Planck radiation of a body at ambient temperature was entered to approximately 98 %. For a number of polymer films transmission data in the range from 400 to 4000 cm⁻¹ were also determined using two different FT-IR spectrometers of the type PE1600 (Perkin Elmer; Überlingen, D) and IFS66v/S (Bruker; Ettlingen, D), the latter being evacuated for increased accuracy. In all cases, excellent agreement in spectral results was obtained for the three devices.

3.2 Calculation Procedure

The procedure to calculate the integral solar absorption coefficient, κ^S , and the scattering coefficient, σ^S , starting from the spectral transmittance and reflectance data is illustrated

Table 1. Investigated polymer film types (polymer nomenclature; polymer morphology (amorphous, a, or semicrystalline, sc), index of refraction; maximum long term service temperature; film thickness; film production process (casting, c, or extrusion, e)

Polymer type	Abbrev.	Morphology	Serv.Temp. [°C]	Index of Refr.	Thickness [μm]	Production
Cellulose acetate	CA	a	80	1.49	30 – 100	c
Cellulose triacetate	CTA	a	100	1.49	30 – 125	c
Polycarbonate	PC	a	120	1.59	50 – 135	e / c
Polycarbonate copolymer	PC-HT	a	160	1.57	40	e
Polyethyleneterephthalate	PET	sc	100	1.58	5 – 100	e
Polyethylenenaphthalate	PEN	sc	150	1.58	75	e
Polymethylmethacrylate copolymer	PMMA	a	80	1.49	50 – 125	e
Ethylenecycloolefine copolymer	COC	sc	110	1.53	35	e
Polymethylpentene	PMP	sc	120	1.46	25 – 100	e
Polypropylene	PP	sc	100	1.47	30	e
Ethylene-tetrafluorethylene copolymer	ETFE	sc	150	1.40	12 – 150	e
Tetrafluorethylene-perfluoro-propylene copolymer	FEP	sc	200	1.34	12 – 122	e
Perfluoro-alkoxy copolymer	PFA	sc	260	1.35	50 – 102	e
Fluoro-alkoxy terpolymer	TFA	sc	130	1.35	80 – 100	e
Polyetheretherketone	PEEK	sc	200	1.58	50 – 100	e
Polyetherimide	PEI	a	170	1.70	25 – 100	e

schematically in Fig. 1.

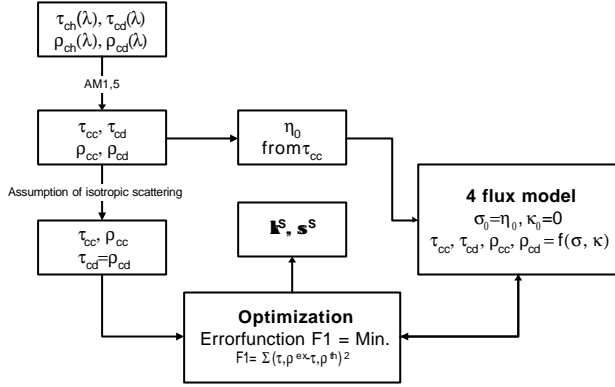
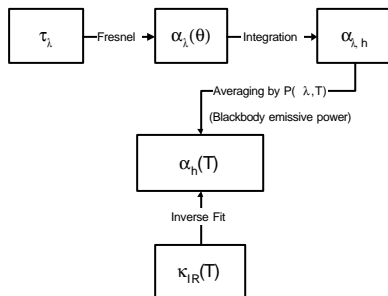


Fig. 1. Calculation procedure for the integral solar absorption coefficient, κ^S , and the solar scattering coefficient, σ^S .

At first the collimated-collimated transmittance and reflectance values were calculated subtracting the collimated-diffuse data from the collimated-hemispherical data. The spectral averages (or integral data) were determined by weighting the measured spectral radiometric property such as transmittance or reflectance by the AM 1.5 Global Irradiance source function. Due to the fact that radiation outside a cone of approximately 5° belonged to the diffuse component and because of the small differences between diffuse reflectance and diffuse transmittance (the difference was in many cases less than 0.01), isotropic scattering was assumed and the transmittance and reflectance data were adapted appropriately. On the one hand, these experimental integral properties were input data for the optimization routine. On the other hand, the 4-flux model (a generalization of the Maheu model (Maheu et al., 1984)) was used to calculate theoretical transmittance and reflectance values as a function of the integral absorption and scattering coefficients. In order to apply the 4-flux model, a number of parameters appearing in the theory must be known. The forward scattering ratio for both, collimated and diffuse light, was kept constant at 0.5. The average pathlength parameter for diffuse flux was defined as 2.0. The 4-flux model calculations gave theoretical values for the following four parameters: collimated-collimated transmittance, τ_{cc} , collimated-diffuse transmittance, τ_{cd} , collimated-collimated reflectance, ρ_{cc} , and collimated-diffuse reflectance, ρ_{cd} . Subsequently, the error function, that is the sum of the quadratic differences between experimental and theoretical values, was minimized and the variables κ^S and σ^S were optimized numerically. As starting parameters the absorption coefficient was defined as 0, and the scattering coefficient was set equal or larger than the overall extinction coefficient calculated from the experimental τ_{cc} value.



The procedure for determining the integral IR absorption coefficient, κ_{IR} , starting from the spectral transmittance data is shown in Fig. 2.

Fig. 2. Calculation procedure for the effective infrared absorption coefficient, $\kappa_{IR}(T)$.

The directional spectral absorptance, $\alpha_{\lambda}(\theta)$, was calculated for both transverse electric and transverse magnetic polarization using the spectral collimated-collimated transmittance, the film thickness and the constant index of refraction as input parameters according to Rubin (Rubin, 1982). The hemispherical spectral absorptance, $\alpha_{\lambda,h}$, for unpolarized radiation was found by ideally directional averaging with 5° steps and averaging over both polarization directions. Finally, the total hemispherical absorptance, $\alpha_h(T)$, was determined by averaging the spectral values, weighted by a blackbody emissive power, $P(\lambda,T)$, at each wavelength. The temperature was varied between 10 and 100°C . The effective temperature dependent absorption coefficient, $\kappa_{IR}(T)$, was found by an inverse fit. Although κ_{IR} in general is temperature dependent, in this paper the absorption coefficient, κ_{IR} , for 20°C only is described and discussed, as this temperature is of special relevance for TI wall applications.

4. RESULTS AND DISCUSSION

In the following the solar optical properties and the infrared radiative properties will be described and discussed separately. Due to restrictions in space only selected data sets are presented, which, however, are representative of the various molecular and microstructural effects observed.

4.1 Solar Optical Properties

The collimated-hemispherical and collimated-diffuse transmittance spectra for $50\ \mu\text{m}$ thick films of PC and FEP are shown in Fig. 3. The different collimated-hemispherical transmittance values, τ_{ch} , are a result of the different indices of refraction, which are 1.59 and 1.34 for PC and FEP, respectively. Due to dispersion effects the τ_{ch} values are slightly decreasing at shorter wavelengths. In the near UV range (300 to $400\ \text{nm}$), PC shows a pronounced absorption which can be attributed to electron excitations in interatomic bonds (e.g., double bonds of aromatic ring structures and the carbonyl groups of the polymer chain and/or various bonds of the light stabilizer molecules). While the investigated PC grade contained a UV stabilizer, for FEP (which is inherently light stable and thus contains no light stabilizer) the near UV absorption phenomena are not detected as the fluoride bonds of FEP are not activated in the investigated UV range. Moreover, in the near IR range PC shows moderate absorptions due to vibration activations of C-H and C=O bonds. As the C-F bonds are not activated in this range, no absorptions are observed for FEP.

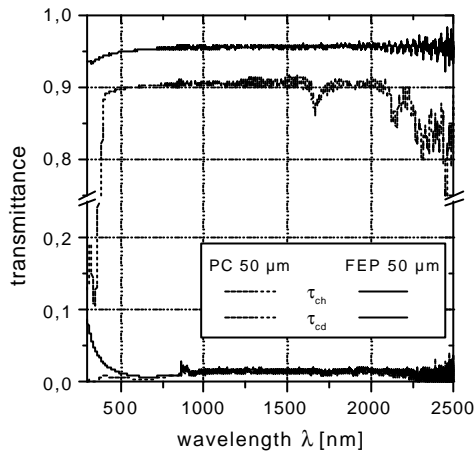


Fig. 3. Collimated-hemispherical and collimated-diffuse solar transmittance (τ_{ch} , τ_{cd}) spectra for 50 μm thick PC and FEP films.

When looking at the diffuse transmittance data in Fig. 3, differences between the PC and the FEP film can be seen at wavelengths less than 500 nm. These are most likely related to the semicrystalline morphology of FEP versus the amorphous microstructure of PC. Thus, for example it could be shown by separate experiments that the dimensions of semicrystalline lamellar band structures in FEP are in range of 30 nm and above, which corresponds to the increase in τ_{cd} below 500 nm.

Averaging the whole solar spectrum from 300 to 2500 nm, absorption and scattering coefficients of 3.0 and 4.2 cm^{-1} , respectively, for first film interactions (single film interaction) were calculated for the 50 μm thick PC film. The extinction coefficient, η_0 , for the single film interaction determined from τ_{cc} and used as approximation for the scattering coefficient in the 4-flux optimization procedure, was found to be 7.2 cm^{-1} . In comparison, a multiple extinction coefficient of 1.0 cm^{-1} was derived from an experimental and theoretical characterization of a lamellar TI structure made from the same PC film. The latter result reflects the fact that, depending on the incident angle, in TI structures a radiation beam passes through successive film elements of the structure (multiple film interactions), before being transmitted through the structure. Due to the strong absorption in the near UV, the integral absorption coefficient for single interaction is valid only for the first interaction between incoming radiation and TI structure. For subsequent interactions, modified coefficients have to be used which neglect the near UV absorption effect. Taking this into account, average values for subsequent scattering and absorption coefficients (following the first interaction) were calculated neglecting the

range of strong absorption during the first radiation/film interaction in the transmittance spectrum. This procedure yields σ^S and κ^S values of 3.1 and less than 0.1 cm^{-1} , respectively, showing a better agreement with TI structure values. Assuming the relevant wavelength spectrum for subsequent interactions, the extinction coefficient, determined from τ_{cc} and used as approximation for the scattering coefficient in the 4-flux optimization procedure, was then found to be 2.3 cm^{-1} , which is in reasonable agreement with the extinction value of 1.0 cm^{-1} obtained from the TI structure.

For the 50 μm thick FEP film integral scattering and absorption coefficients of 4.4 and less than 0.1 cm^{-1} , respectively, were calculated as average over the whole solar spectrum. Neglecting the near UV range (300 - 400 nm) yielded only a minor change of the σ^S value to 4.0 cm^{-1} . In other words, for polymer films with rather moderate peaks in the transmittance spectra, a distinction between single and subsequent film interactions may be neglected.

Based upon the considerations and the procedure just described, the effect of film thickness, Z , on the relevant solar scattering coefficient, σ^S , is shown for several low and high temperature polymer films in Fig. 4 and 5, respectively. This procedure yielded absorption coefficients of less than 0.1 cm^{-1} for all investigated polymer films, so that no separate illustration seems necessary.

Figures 4 and 5 show that the solar scattering coefficients of the polymer films investigated range from 1.3 to 13.9 cm^{-1} , with scattering contributing more than 99 % to the solar extinction coefficients. Apart from the semicrystalline FEP and PET films, which compare well with amorphous polymer films, the semicrystalline polymer films in general reveal a higher degree of extinction or scattering. To obtain such excellent solar extinction properties with the semicrystalline polymers, the polymer films have to be stretched following the extrusion process or by post-processing to yield a fine crystalline microstructure. However, when applying such films in higher temperature applications the possibility of post- and recrystallization needs to be taken into account. In fact, the higher scattering coefficients of ETFE compared to FEP are probably due to the higher degree of crystallinity and larger lamellar dimensions of the former.

In addition to the microstructure, the addition of various additives may play a significant role. To achieve excellent solar optical properties, processing additives frequently used in the production of polymer films, such as antiblocking and antistatic agents, should be avoided. While no information is available as to the use of processing additives for PMP, for the other three semicrystalline polymers (PET, ETFE, FEP) no antiblocking and antistatic agents were used.

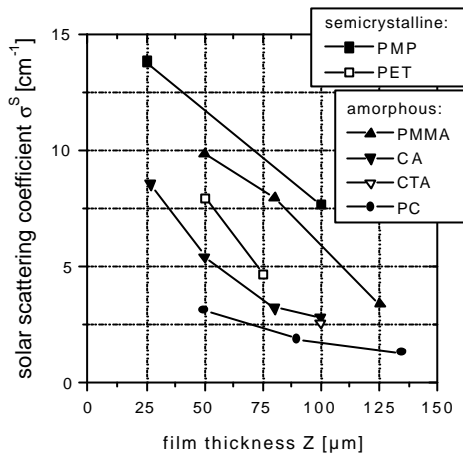


Fig. 4. Solar scattering coefficient, σ^S , of transparent polymer films with service temperatures of approx. 100 °C as a function of film thickness, Z (single film interaction for PMP, CA, CTA; subsequent film interactions for PET, PMMA, PC).

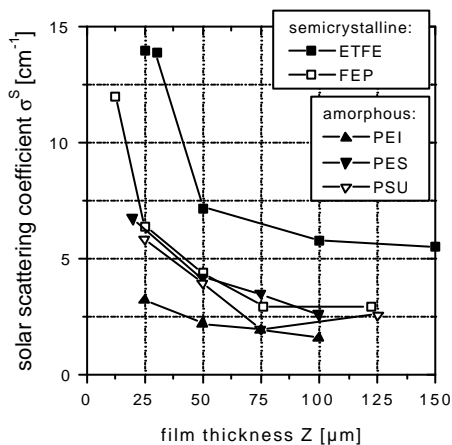


Fig. 5. Solar scattering coefficient, σ^S , of transparent polymer films with service temperatures ranging from 150 to 200 °C as a function of film thickness, Z (single film interaction for ETFE, FEP; subsequent film interactions for PEI, PES, PSU).

Differences in the solar scattering coefficients were also found for the amorphous polymer films, especially when comparing the low temperature polymer films of PC, CA and PMMA in Fig. 4. While some of these differences are of course related to the molecular structure of these polymers, the inclusion of additives and modifiers in amorphous polymers may also play a role. From the three materials just mentioned, PC contains a UV stabilizer and CA is modified with a plasticizer and an SiO₂ antiblocking agent. Due to the brittleness of PMMA homopolymer, the PMMA films were produced from an impact modified copolymer grade (using butylacrylate as comonomer) with improved tearing resistance. In general, the optical properties of such materials depend on the size (including the

size distribution), the content and the distribution of particles and second phase structures and their difference in the index of refraction compared to the base polymer. While Fig. 4 reveals a significant difference in optical properties between PMMA and PC, there are also PMMA grades with equivalent solar optical properties to PC available.

The increase in solar scattering coefficients with decreasing film thickness is primarily a result of the increasing contribution of surface scattering effects for thinner polymer films. For a film thickness of 50 μm it was found by best fit calculations, that surface scattering contributes between 50 and 70 % to the total scattering for many polymer films, depending on the polymer type. Further investigations using atomic force microscopy in an appropriate bandpass are currently being performed to further study the influence of geometrical surface characteristics on the solar scattering coefficient of transparent polymer films. First results indicate a reasonable correlation between rms-roughness and the dimensionless solar scattering coefficient ($\sigma^S \cdot Z$).

3.2 Infrared Radiative Properties

The excitation of vibrations of certain molecular groups in the IR range takes place only, if the electric dipole moment changes as a result of the change in the charge distribution. Thus, only an oscillating dipole will interact with the electromagnetic field by absorption of energy. The medium IR range can be divided into two regions. The range between 4000 and 1000 cm⁻¹ contains mainly fundamental bands of functional groups or interatomic bonds as well as many usually weak overtones and combinations. These fundamental bands are often only slightly influenced by the rest of the molecule. In the range from 1000 to 200 cm⁻¹, however, induced motions in larger groups or molecular segments of polymeric molecules are responsible for absorption bands.

The collimated-collimated transmittance spectra for 50 μm thick PC and FEP films are shown over the medium IR range in Fig. 6. Close to 1000 cm⁻¹, the wavenumber at which the blackbody emissive power function at 20 °C contains a maximum, both, PC and FEP show intensive absorption bands due to C-O (ether) and C-F (fluoride) bonds, respectively. In addition, imide-, sulphone- and siloxane-groups are of major relevance for extinctions in polymers in the medium IR range. Polymers, such as polyolefines (e.g., polyethylene (PE), polypropylene (PP) or PMP), which consist of C and H atoms only, reveal the lowest absorption in medium IR range.

Returning to Fig. 6 it should be noticed, that several of the absorptions for 50 μm films apparently are too strong to be resolved spectrally. Not even for a 12.7 μm thick FEP film (the smallest film thickness investigated), the C-F absorption bands could be resolved.

Infrared absorption coefficients for various polymer films are plotted for low and high temperature polymer films as a function of film thickness in Figs. 7 and 8, respectively. The κ_{IR} values of the polymer films investigated were found to range from 19.2 to 328.4 cm⁻¹, with the polyolefine PMP exhibiting

the lowest and the modified cellulose based polymers (CA, CTA) revealing the highest values for infrared absorption. The high absorption coefficients of CA and CTA are predominantly a result of the high density of C-O bonds in the molecular structure of these polymers. While the low temperature polymer film types of PET, PMMA and PC also contain C-O groups, compared to the cellulose based films their density is significantly lower. Consequently, with regard to their infrared absorption coefficients, PET, PMMA and PC films were found to be positioned in the midrange between PMP and CA/CTA (see Fig. 7).

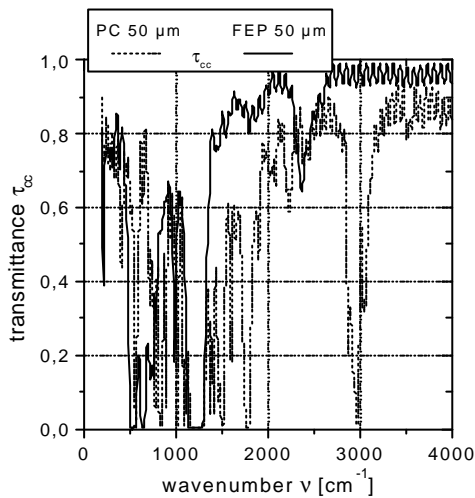


Fig. 6. Collimated-collimated infrared transmittance, τ_{cc} , spectra for 50 μm thick PC and FEP films.

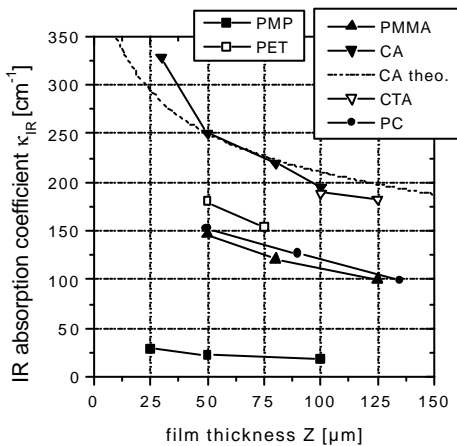


Fig. 7. Infrared absorption coefficient, κ_{IR} , of transparent polymer films with service temperatures of approx. 100 $^{\circ}\text{C}$ as a function of film thickness, Z .

For κ_{IR} values of the high temperature polymer films shown in Fig. 8, the following ranking was obtained: FEP < ETFE, PSU < PES < PEI. For these films the range covered by the various film types is much reduced due to their molecular architecture. Although different in their chemical nature and in the degree of

freedom of mobility, all these polymer types contain a certain density of IR absorbing groups (fluoride, sulphone, ether and imide groups), thus yielding κ_{IR} values in the upper range of those covered by the low temperature films of Fig. 7.

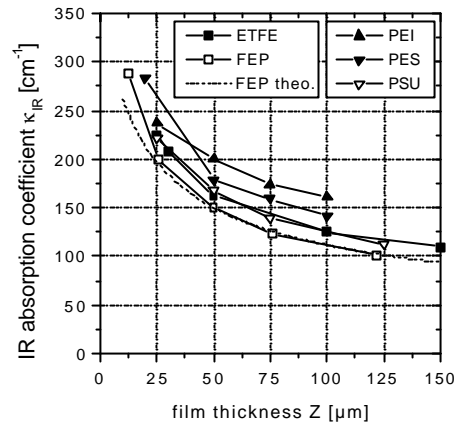


Fig. 8. Infrared absorption coefficient, κ_{IR} , of transparent polymer films with service temperatures ranging from 150 to 200 $^{\circ}\text{C}$ as a function of film thickness, Z .

From Figs. 7 and 8 it may also be noted, that the κ_{IR} coefficients for all polymer films were found to increase progressively as the film thickness is reduced. This is in good agreement with previous investigations of PET films by Rubin (Rubin, 1982), who found that the hemispherical emittance values increase progressively with thickness combined with the model description of the interdependence of hemispherical emittance, infrared absorption coefficient and thickness based on the Fresnel equations. In fact, the dashed curves in Figs. 7 and 8 represent theoretical approximations of the κ_{IR} vs. film thickness dependence, for CA and FEP, respectively, calculated using the transmittance spectrum of 50 μm film as reference. While in general rather good agreement was found between experimental and theoretical curves, some differences apparently exist especially for small thickness values. This may possibly be explained by local film thickness variations, stronger interference effects of thinner polymer films and errors due to strong absorption at C-O and C-F bands which cannot be resolved fully.

REFERENCES

- Graf R. T., Koenig J. L., Ishida H. (1985). Optical constant determination of thin polymer films in the infrared. *Applied Spectroscopy*, Vol. 39, No. 3, 405-408
- Maheu B., Letoulouzan J. N. and Gouesbet G. (1984). Four-flux models to solve the scattering transfer equation in terms of Lorenz-Mie parameters. *Applied Optics*, Vol. 23, No. 19, 3353-3362

Neidlinger H. H. (1987). The effect of the size of structural bulk inhomogeneities on the specular transmittance of polymer films. *Solar Energy Materials* 16, 393-402

Platzer W. J. (1992). Directional-hemispherical solar transmittance data for plastic honeycomb-type structures. *Solar Energy*, Vol. 49, No. 5, 359-369

Rubin M. (1982). Infrared properties of polyethyleneterephthalate films. *Solar Energy Materials* 6, 375-380